

A TWO-ELEMENT MICROMACHINED MICROSTRIP ANTENNA ARRAY WITH IMPROVED PERFORMANCE

Arun V Sathanur and K.J. Vinoy

*Microwave Laboratory
Department of Electrical Communication Engineering
Indian Institute of Science, Bangalore 560 012. INDIA
Tel. +91 (80) 2293 2853. Email: kjvinoy@ece.iisc.ernet.in*

I. INTRODUCTION

Various micro-electromechanical and micromachined systems and components are expected to form a significant share of telecommunications equipment in the very near future [1]. Antenna being an efficient interface between electronic circuits and the outside world, is an important component in any wireless communication system. In keeping with the trend towards using higher frequencies in modern communications applications, (e.g., space applications at around 30GHz, local multipoint distribution systems (LMDS) at 28 GHz) antenna technology needs to meet new requirements. The *Microwave Lab.* at the Indian Institute of Science has been engaged in the development of various subsystems for such an active monolithic phased array antenna operational at 30 GHz.

The antenna configuration that finds applications in several telecommunications systems is based on microstrip technology. The microstrip patch antenna consists of a metallic patch on a grounded dielectric slab such that the length of the patch is approximately half the guided wavelength. This is a low profile antenna, highly preferred for space applications due to light weight and conformability. However, this suffers from low bandwidth and reduced radiation efficiency especially when fabricated on high dielectric constant substrates such as GaAs or Silicon. Furthermore, microstrip antennas, although currently used in several microwave bands, can not be easily scaled to mm wave bands. Many micromachining approaches can therefore be employed to overcome these difficulties.

Micromachining assumes great significance in the context of the high level of system integration required at the mm wave bands. If a large number of components should be integrated into circuits at chip levels, semiconductor substrates should themselves be used for antennas. The advantages of using GaAs and Silicon substrates in the context of monolithic microwave integrated circuits (MMICs) are widely understood. Although GaAs is a good substrate for microwave circuits, antennas on them suffer from low bandwidth and degraded radiation characteristics due to its high dielectric constant [2] [3]. Developing micromachining technology is therefore essential for integrating an entire communication system on a chip.

Most of the results so far on micromachining have been restricted to silicon, albeit this is not so much preferred at millimeter wave frequencies [4]. However most of the current MMIC fabrication processes are on GaAs. Hence in this study we examined the usefulness of micromachining concepts to GaAs based antenna systems. The advantages of micromachining in microstrip patch antennas are multifaceted. In a single patch scenario, this approach can effectively reduce the effective dielectric constant of the substrate by selectively removing material (e.g., underneath the patch) and thus improve its bandwidth and radiation efficiency. We have recently demonstrated these improvements in a single-patch scenario [5]. However in the context of antenna arrays, trenches or cavities can be micromachined below or between patches to improve the overall performance. The present work starts out by outlining an approach for designing single element patch antennas on micromachined GaAs substrate and then extends this to design a 2x1 array.

II. DESIGN OF PATCH ELEMENT ON MICROMACHINED GaAs SUBSTRATE

Starting with preliminary expressions in [6] we designed a patch element on a GaAs substrate compatible with MMIC technology, having a dielectric constant of 12.9 and thickness of 350 μm . After fine-tuning the dimensions to make the antenna resonate at 30GHz, the patch length and width are obtained as 1.21 mm and 1.91 mm, respectively. A 50 Ω microstrip line is used to feed the antenna which is matched by means of an inset [6]. A commercial time domain code is used for the simulations. It maintains at least 15 cells per wavelength at the shortest wavelength to ensure good accuracy. Important antenna parameters are extracted during post processing.

The antenna is re-designed on the micromachined substrate. In order to obtain maximum benefits of micromachining and ensure that the wafer does not break, we designed the antenna for an etch depth of 300 μm leaving 50 μm of GaAs. The etch profile with sloping walls inclined at 55° has been used in the geometry input to the full wave simulator. This profile is true for Silicon wafers. Although the profile is not so well defined for

GaAs, and we can not take into account all the irregularities, this is used as a limit case. The antenna geometry (with some dimensions exaggerated for clarity) is shown in Fig. 1.

For designing the micromachined antenna, we needed to determine the synthesized dielectric constant of the composite substrate consisting of the air and the GaAs layers. It may be recalled that the transmission line model for the design of microstrip antennas treats the patch as a microstrip line of a particular width and obtains the effective permittivity by using the well known formula for $\epsilon_{r_{eff}}$ for a microstrip line. In order to extract the effective permittivity, we simulated the scenario of propagation through a microstrip line on the composite substrate which models appropriate extension of the cavity beyond the width of the line strip. In a microstrip line, properties like characteristic impedance and effective dielectric constant depend on the width of the line and, in this particular case, the dimensions of the cavity below the strip. Simulations have been performed for several cases where the cavity extends by incremental steps between $2h$ to $6h$ beyond the microstrip line width in either directions. The propagation constant will yield the effective synthesized permittivity. The synthesized permittivity is obtained from the well known microstrip effective permittivity formula:

$$\epsilon_{r_{synth}} = 1 + 2 \frac{\sqrt{1 + \frac{12h}{w}} - 1}{\sqrt{1 + \frac{12h}{w}} + 1} \epsilon_{r_{synth_{eff}}} \quad (1)$$

where $\epsilon_{r_{synth_{eff}}}$ is the effective synthesized permittivity defined by

$$\epsilon_{r_{synth_{eff}}} = \left(\frac{k_0}{\beta} \right)^2 \quad (2)$$

where k_0 is the free space wave number at the frequency of interest and β is the propagation constant for the propagation along the microstrip line. Fig. 2 shows the variation of the synthesized permittivity of the composite substrate with microstrip width for two different extensions of cavity beyond the microstrip in the width direction. These optimizations for the resonance at 30 GHz gave the patch length as 3.62 mm.

We further define a figure of merit based on the Gain-Bandwidth product and optimized the cavity dimensions for the best FOM. This resulted in the cavity extensions of $1.3H$ and $6.7H$ in the length and width directions and the optimum gain obtained was 9.1dB and the bandwidth was 1.48 GHz. This was a great improvement over the patch on the plain substrate which exhibited 911 MHz bandwidth, 4dB gain and 69% radiation efficiency. Further the E-Plane pattern which shows an off-boresight main beam possibly due to the surface waves diffracting off the edges of the substrate is totally absent in the micromachined case. All these improvements are evident from figures 3 and 4.

III. 2x1 ARRAY ON MICROMACHINED GaAs SUBSTRATE

The present work concentrates on a two-element array with a single cavity under the patches. The cavity is extended in both the directions by $1.6H$ and $6.7H$ as outlined in section II. This schematic is shown in Fig. 5. Simulations are carried out for the patch array on the plain substrate. Then using the optimal patch dimensions for the micromachined case, simulations are carried out for the array on the micromachined substrate. To facilitate comparison we consider center to center separation between patches to be $0.65\lambda_0$ in both the cases. First each element in the array is excited separately and the mutual coupling is investigated. Then both the antennas are simultaneously excited and the radiation pattern for the array is obtained.

First, no feed network is designed and each antenna is excited by an individual port. This allows us to examine the mutual coupling by means of S_{21} . It appears from figure 4 that the mutual coupling has not been reduced by micromachining. This is mainly due to the fact that, micromachining increases the dimensions of the radiating element and hence the physical separation between adjacent patch edges becomes quite small and mutual coupling increases. However, a 0.8dB worsening is quite small compared to the other benefits accrued.

However if the elements are separated so that the separation between the edges is kept at the same value as the array on the plain substrate case, a 3dB improvement in mutual coupling has been obtained at the resonant frequency. The mutual coupling plot for all three cases is shown in figure 5.

Next a corporate feed network is designed for simultaneously exciting these patches from a common port using standard procedure. The 50Ω feed line is split into two 100Ω ones, each going over to an antenna. Quarter wave transformers are then used to match these lines to the antenna elements themselves. The bends in the line are chamfered to avoid sharp discontinuities. From the resulting simulations, S_{11} , bandwidth, directivity and radiation efficiency have been determined. The comparison of important parameters is shown in the Table 1. The return loss plots are quite similar to that of the single element case and are not shown. The radiation patterns in principal planes are also shown in figures 6 and 7. We can see that micromachining restores the main beam along boresight in the E-Plane. The antenna array on the micromachined GaAs exhibits a 3.4 dB

improvement in directivity, 17% improvement in radiation efficiency and 61% increase in bandwidth. The improvements in radiation characteristics may be attributed to the reduction in surface wave modes with the reduction in the synthesized dielectric constant.

IV. CONCLUSIONS

Micromachining is shown to improve the performance of antenna arrays on GaAs substrate. The bandwidth improvement obtained for single element antenna is available in the array scenario as well. All important antenna parameters like gain, bandwidth and radiation efficiency are seen to improve. The antenna array on the micromachined GaAs exhibits a 3.4 dB improvement in directivity, 17% improvement in radiation efficiency and 61% increase in bandwidth. Further the overall shape of the radiation pattern is also improved which may be attributed to the suppression of surface waves by micromachining.

REFERENCES

- [1] V.K. Varadan, K.J. Vinoy and K.A. Jose, *RF MEMS and their applications*, John Wiley, London, 2003
- [2] D.M. Pozar, "Considerations for millimeter wave printed antennas," *IEEE Trans. Ant. & Propagat.*, vol 31, pp. 740-747, 1993.
- [3] D.M. Pozar, "Rigorous closed-form expressions for the surface wave loss of printed antennas," *Electron. Lett.*, vol. 26, pp. 954-956, 21 June 1990.
- [4] Papapolymerou, I.; Franklin Drayton, R.; Katehi, L.P.B., "Micromachined patch antenna," *IEEE Trans. Ant. & Propagat.*, vol. 46, pp. 275-283, 1998.
- [5] S.V. Arun, R.S. Khetrimayum, and K.J. Vinoy, "Performance enhanced micromachined patch element for monolithic GaAs based active phased array antenna," International Conf. on Antenna Technologies, February 23-24, Ahmedabad, India, 2005
- [6] C.A. Balanis, *Antenna Theory: Analysis and Design*, John Wiley, New York, 1997

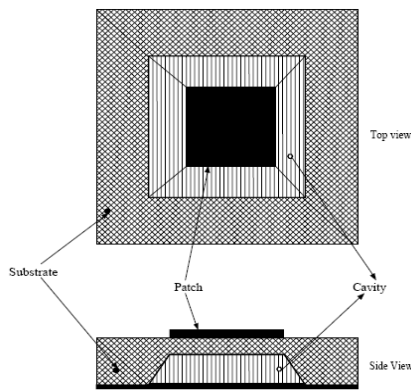


Fig. 1 Schematic of a single element patch antenna

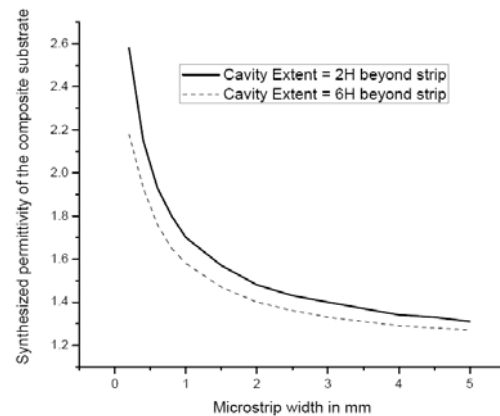


Fig 2 : Effective synthesized permittivity

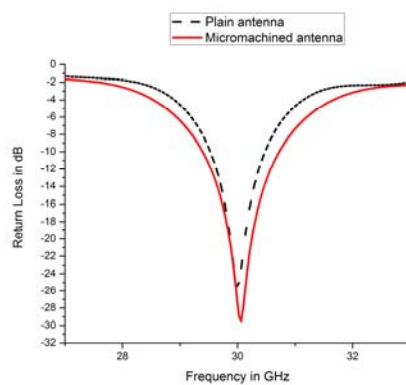


Fig 3 : S_{11} bandwidths compared

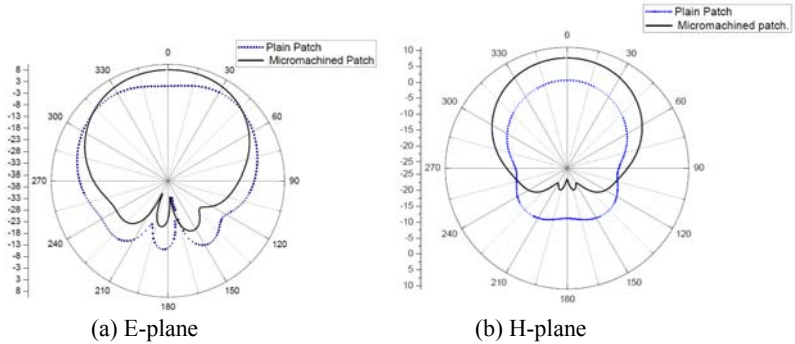


Fig. 4 Radiation patterns of single element antenna

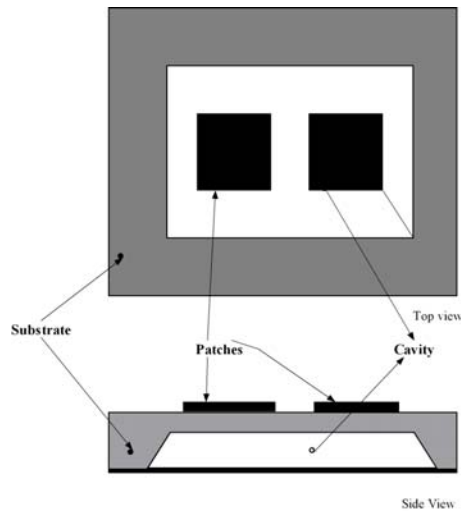


Fig 5 : Micromachined patch antenna array.

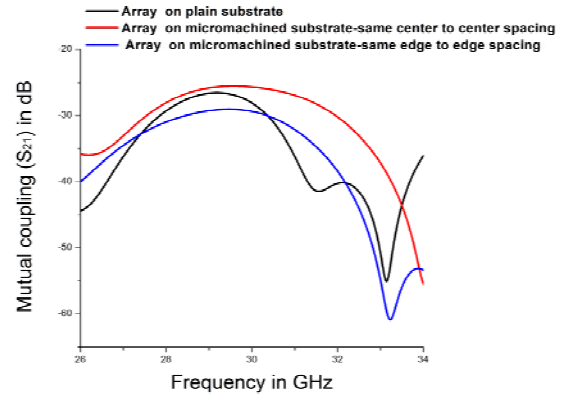
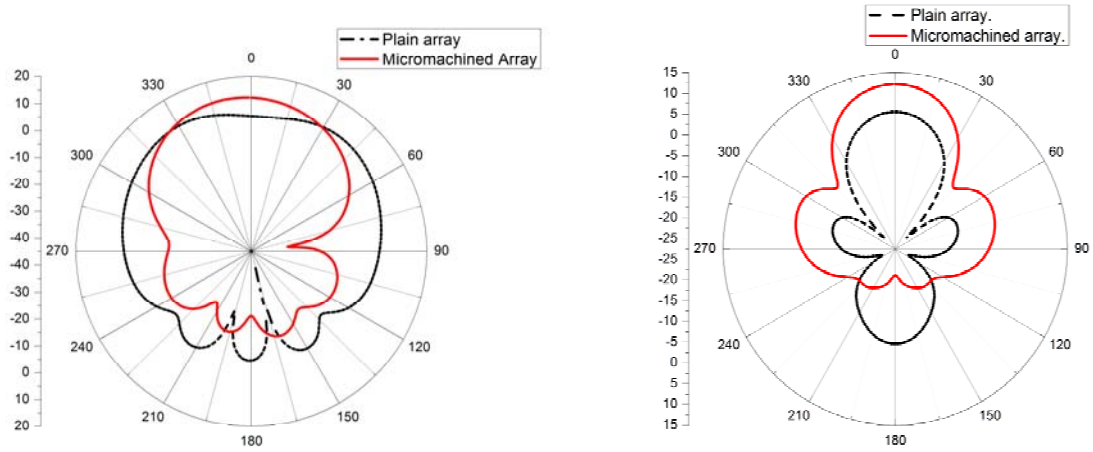


Fig 6: Comparison of mutual coupling of various array configurations.



(a) E-Plane patterns

(b) H-Plane patterns

Fig. 7 Radiation patters of the antenna arrays on micromachined and plain substrates

Table 1: Comparison of important parameters of arrays on plain and micromachined substrate.

Important antenna parameters	Array on plain GaAs substrate	Array on micromachined GaAs substrate
S11 bandwidth	887 MHz	1426 MHz
Directivity	9.2 dB	12.6 dB
Efficiency	63%	80%
Gain	7.2 dB	11.6 dB
S21	-26.5 dB	-25.7 dB